Biochemical and Thermodynamic Characterization of Compounds That Bind to RNA Hairpin Loops: Toward an Understanding of Selectivity†

Jason R. Thomas, Xianjun Liu, and Paul J. Hergenrother*

Department of Chemistry, Roger Adams Laboratory, University of Illinois, Urbana, Illinois 61801

Received April 14, 2006; Revised Manuscript Received July 11, 2006

ABSTRACT: Elucidation of the molecular forces governing small molecule−RNA binding is paramount to the progress of rational design strategies. The extensive characterization of the aminoglycoside−16S rRNA A-site interaction has deepened our understanding of how aminoglycosides bind to their target and exert their antimicrobial effects. However, to date no other RNA binding compounds have undergone such rigorous evaluation, and in general the origins of small molecule−RNA binding remain a mystery. We recently reported the identification of small molecules, dimers of 2-deoxystreptamine, which are able to bind selectively to RNA tetraloops and octaloops, respectively [Thomas, Liu, and Hergenrother (2005) *J. Am. Chem. Soc. 127*, 12434−12435]. Described herein is the biochemical and biophysical characterization of the RNA binding properties of the most selective compound, **B-12**, as well as closely related analogues. These studies further substantiate that **B-12** is indeed selective for RNA octaloop sequences and indicate that the origin of this selectivity may lie in **B-12**'s unusual binding mode, in which entropic factors are major contributors to the overall binding energy. In fact, isothermal titration calorimetry (ITC) experiments indicate that the binding of **B-12** and most of its analogues is associated with a strong entropic contribution to the total binding energy. This is in stark contrast to the aminoglycosides, for which favorable enthalpy typically provides the driving force for binding. These studies are the first to examine small molecule−RNA hairpin loop binding in detail and are a necessary step toward the design of compounds that are specific binders for a given RNA sequence.

Recent estimates suggest that only a subset of the thousands of proteins responsible for disease onset and progression may actually be "druggable", meaning that with current technologies only a small portion of the proteome has appropriate binding pockets for small molecule therapeutics (*1*−*3*). To modulate the function of the ∼85−90% of proteins that cannot be targeted with small molecules, other strategies are needed. Dervan and co-workers have developed a general paradigm for the design of small molecules that target DNA in a sequence-specific manner, allowing for alteration of gene expression (*4*−*7*). Several high-profile success stories have emerged from this work, and the precise scope and limitation of such small molecule−DNA binders are still being defined (*8*, *9*). An alternative approach is the direct targeting of mRNA with small molecules. Single-stranded mRNA folds to produce regions that form both canonical and noncanonical base pairs, resulting in hairpin loops, internal loops, and bulges. These unique RNA secondary structures are thought to provide suitable pockets for binding to small molecules (*10*). Using small molecules to directly target mRNA could provide a complementary means to modulate protein levels, provided that compounds that are selective for a particular message from the transcriptome could be developed (*10*−*15*).

A naturally occurring system demonstrating the druggability of transcripts is that of the riboswitch. Riboswitches are a class of mRNAs which harbor a binding site for a small molecule metabolite in either the 5′ untranslated region (UTR) or 3′-UTR; the small molecule binding event regulates translation (*16*−*28*). These regulatory RNAs consist of an aptamer domain (the ligand binding site) and an expression platform (the region that undergoes conformational change to alter translational efficiency). The aptamer domains demonstrate exquisite specificity and have a range of binding affinities [1 nM (*20*) to 30 μM (*22*)] for their respective ligands. This combination of high specificity and strong binding affinity allows riboswitches to perform central tasks in many biochemical pathways by means of ligand-induced allosteric changes in the mRNA conformation. The clinical utility of the aminoglycosides also has demonstrated that RNA is indeed a druggable target (*12*, *14*). These antibiotics target the A-site decoding region of the 16S rRNA present in prokaryotes. As antimicrobial agents, the aminoglycosides have been in use in the clinic for over half a century and have enjoyed varying degrees of success, with their ototoxicity and nephrotoxicity placing limits on their broader application (*29*).

On the basis of the success of the aminoglycosides and the discovery of riboswitches, there is little doubt that targeting RNA could be a viable therapeutic strategy. However, examples where exogenously added small molecules are used to selectively target a given mRNA in a cellular context are extremely rare (*30*, *31*). This is likely

† This work was supported by the National Institutes of Health (NIGMS R01-GM68385). P.J.H. is a fellow of the Alfred P. Sloan Foundation.

* Corresponding author. E-mail: hergenro@uiuc.edu. Phone: (217) 333-0363. Fax: (217) 244-8024.

10.1021/bi0607296 CCC: $33.50
Published on Web 08/16/2006

because small molecules discovered during in vitro experiments have a propensity to bind multiple RNA targets of unrelated sequence and structure (*32*−*37*); specifically, the promiscuity of aminoglycosides is generally attributed to their ability to undergo conformational adaptation with highly flexible RNA binding pockets, thus allowing them to fit into a variety of RNA binding sites (*11*, *13*). Generally, RNA binding small molecules associate to regions of the RNA A-form helix that are perturbed by mismatched base pairs (*10*). RNA binding small molecules (such as aminoglycosides) tend to bind internal loops and bulged regions (*35*, *36*), while compounds possessing the capacity to bind to hairpin loops are comparatively rare (*38*−*41*).

The current understanding of the fundamentals of small molecule−RNA interactions is derived nearly exclusively from studies with aminoglycosides; among these, the aminoglycoside−16S rRNA A-site interaction is the best characterized system. Through biochemical analysis, electrostatic interactions were determined to play a primary role in aminoglycoside−RNA binding. In a series of papers, Pilch and co-workers explicitly determined that aminoglycoside protonation is coupled with complexation and that enthalpy is the major contributor to the total binding energy at physiological pH; entropic factors become important at pH 5.5 (*42*−*44*). Beyond biochemical and biophysical characterization, structural data [NMR (*45*) and crystallographic (*46*−*50*)] have unveiled the diverse array of direct and water-mediated contacts between the aminoglycosides and the A-site.

Far less progress has been made with non-aminoglycoside small molecules. As such, it remains unclear if the lessons learned from the 16S A-site studies are directly transferable to other aminoglycoside−RNA interactions, let alone those involving non-aminoglycoside small molecules. We have previously disclosed the first class of small molecules, dimers of 2-deoxystreptamine (DOS dimers),[1] which display general hairpin loop binding properties (*40*). From this initial design a focused combinatorial library of bistriazole DOS dimers was synthesized, and from this library of 105 compounds, five were identified as selective ligands for RNA octaloops relative to RNA tetra-, hexa-, and heptaloops (*41*).

Hairpin loops are a predominant and functionally significant class of RNA secondary structures, as they provide sites of nucleation for RNA folding (*51*), and participate in RNA−protein (*52*, *53*) and RNA−RNA interactions (*54*). The prevalence of RNA hairpin loop size and sequence is likely related to its thermodynamic stability. Based solely on hairpin loop size hexa- and heptaloops have been determined to be the most thermodynamically stable, as six to seven nucleotides present the ideal length for spanning the A-form helix (*51*, *55*). However, the sequence of hairpin loops can greatly contribute to the overall stability. Several RNA hairpin loops smaller than hexaloops have been identified to be significantly more stable than expected by nearest neighbor calculations. The UUCG (*56*), GNRA (*57*), and YNMG (*58*) tetraloops are representative cases of primary sequence dictating hairpin loop stability; such exceptionally stable hairpin loops are frequently observed motifs in RNA folding (*51*). RNA hairpin loops of eight or more nucleotides are penalized by unfavorable entropy of loop formation; thus, large hairpin loops are significantly less stable than those previously mentioned (*51*, *55*). Due to their decreased stability, larger RNA hairpin loops are less frequently observed and are thus relatively unique molecular targets for exploitation by small molecules.

Described herein are experiments aimed at understanding the origins of small molecule−RNA loop size selectivity by testing the most selective compound, **B-12**, and closely related analogues (**B-11**, **B-13**, and **B-14**) (see Figure 1A) in a myriad of biochemical and biophysical assays. From these experiments we were able to determine that the DOS dimers tested generally exhibit no pH dependence of binding, have a greatly reduced contribution of electrostatic free energy (ΔG_{elec}) to the total free energy (ΔG_{total}) of binding, and bind to RNA octaloops in an entropically driven fashion at physiological pH. These results are in distinct contrast to previous studies performed with the aminoglycoside−16S rRNA A-site system (*42*−*44*), thus emphasizing that the understanding of RNA−ligand interactions remains incomplete and that truly RNA structurally specific small molecules will likely have properties considerably different from their nonselective aminoglycoside counterparts.

MATERIALS AND METHODS

Materials. All reagents were obtained from Fisher unless otherwise stated. All solutions were made with Milli-Q purified water. All RNAs utilized in binding assays were purchased from Dharmacon Research with a 3′-terminal fluorescein modification. The *Escherichia coli* tRNA mixture was purchased from Fluka. DOS dimers were synthesized as described (*41*).

Fluorescence Binding Assay. The ligand solutions were prepared as serial dilutions in TM1 buffer (10 mM Tris, 1 mM $MgCl_2$, pH 7.5) at a concentration four times greater than the desired final concentration to allow for the subsequent dilution during the addition of the RNA solution. The appropriate ligand solution (25 μL) was then added to a well of a black 96-well plate (Nunc 237105). Refolding of the RNA was performed using a thermocycler as follows: The RNA, stored in 10 mM Tris and 0.5 mM EDTA, pH 7.5, was first denatured by heating to 95 °C for 2 min; the temperature was then dropped 0.1 °C/s until the temperature reached 25 °C. After refolding, the RNA was diluted to a working concentration of 37.5 nM through addition of the appropriate amount of TM1 buffer (<4 μL added into 1900 μL of buffer). The tube was mixed by inversion, and then 75 μL of the RNA solution was added to each well containing ligand. This dilution brought the final RNA concentration to 28 nM. The fluorescence was measured on a Criterion Analyst AD (Molecular Devices) with an excitation filter of 485 ± 15 nm, an emission filter of 530 ± 15 nm, and a 505 nm dichroic cutoff mirror. The binding was allowed to proceed to equilibrium, which was monitored in 15 min intervals. Equilibrium was determined when three identical curves were obtained. All curves were fit to a logistic dose−response model using TableCurve 2D v5.01 (eq 8076):

$$y = \frac{a}{1 + (x/K_d)^c}$$

[1] Abbreviations: ITC, isothermal titration calorimetry; DOS dimers, 2-deoxystreptamine dimers.

A)

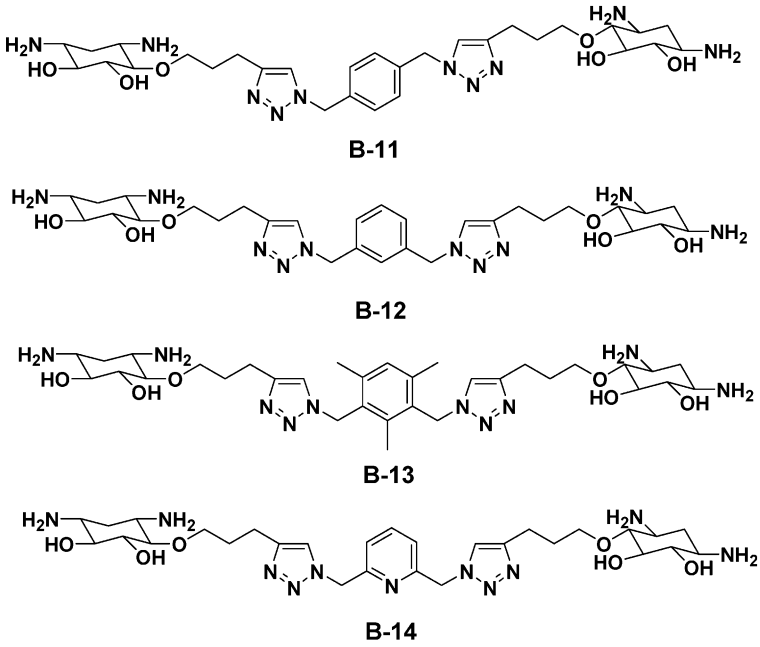

B)

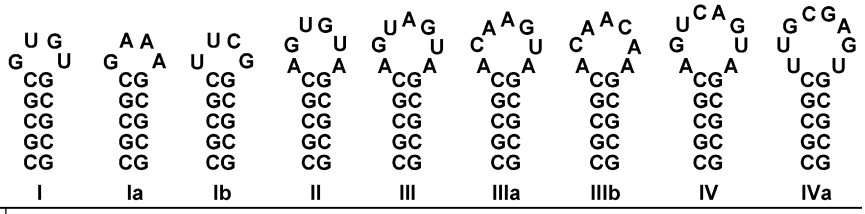

	I	Ia	Ib	II	III	IIIa	IIIb	IV	IVa
B-11	5.73	7.55	6.32	2.07	1.43	2.73	2.03	3.08	2.03
B-12	>25.0*	1.36*	1.54*	10.03*	9.87*	2.23	2.39	0.32*	0.15*
B-13	0.63	0.78	0.84	0.60	2.55	0.44	0.47	0.41	0.48
B-14	5.06	6.08	7.88	4.57	1.27	3.50	3.42	3.00	2.24

FIGURE 1: Size specificity and sequence generality of 2-deoxystreptamine dimer (DOS dimer) binding to RNA hairpin loops. (A) Structures of the compounds utilized in the current study. (B) Dissociation constants for the binding of the DOS dimers to the RNA hairpin loops. All K_d values are listed in μM. All K_d values were determined with the end-labeled method using the RNAs depicted with a fluorescein at their 3′ terminus. The asterisk indicates that the data were previously reported (*41*).

where *a* is the limit that the curve approaches. All binding assays were performed in triplicate. In all cases the error bars on graphs represent one standard deviation from the mean. The tRNA competition experiment was performed as previously outlined (*33*). In brief, a 100-fold excess (base) relative to the fluorescently labeled RNA was refolded in 1900 μL of 10 mM Tris, pH 7.5, 2 mM $MgCl_2$, and 100 mM NaCl at 95 °C for 2 min and allowed to cool to ambient temperature. After the tRNA mixture was cooled, the fluorescence binding assay was carried out as described above with the exception that the fluorescently labeled RNA was added to the refolded tRNA mixture.

pH-Dependent Fluorescence Binding Assay. The pH-dependent binding studies were performed as described in the fluorescence binding assay protocol, above, except that in place of TM1 a buffer consisting of 10 mM Mops and 0.1 mM EDTA was used, and the pH values were adjusted accordingly (*59*).

Ionic-Dependent Fluorescence Binding Assays. Ionic dependence was assessed following the protocol for the fluorescence binding assay except that the final concentration of the NaCl used in each assay was 25, 50, 75, 100, and 125 mM for compounds **B-11**, **B-13**, and **B-14**. For **B-12** the NaCl concentrations used were 100, 200, 300, 400, and 500 mM.

T7 RNAP Expression and Purification. Plasmid pT7-911 was the kind gift of Prof. Scott K. Silverman. An overnight culture of pT7-911 in XLI-Blue (Stratagene) grown in Luria broth (LB)/ampicillin (100 μg/mL) was used to inoculate a 1 L LB/ampicillin (100 μg/mL) culture. This 1 L culture was incubated at 37 °C, 225 rpm, until the OD_{600} reached 0.4−0.6. At this point IPTG was added to the culture to a final concentration of 250 μM, and incubation at 37 °C, 225 rpm, was continued for a period of 4 h. The cells were then harvested by centrifugation at 6000*g* for 30 min. The supernatant was discarded, and the pellet was resuspended in 10 mL of cold binding buffer (10 mM Tris, pH 7.5, 100 mM NaCl, 5 mM β-mercaptoethanol, 5% glycerol, 5 mM imidazole). Cells were lysed by two passages through a French press, at 10000 psi. The lysate was centrifuged at 40000*g* for 30 min. The supernatant was separated from the pellet and incubated with 1.5 mL of Ni-NTA resin slurry (Qiagen) for 1 h at 4 °C. After this batch loading process, the supernatant and Ni-NTA agarose resin were loaded onto an Econo-Pac disposable chromatography column (Bio-Rad). The column was washed with 10 mL of cold binding buffer,

10 mL of cold wash buffer (identical to binding buffer except 10 mM imidazole was added), and the His-tagged T7 RNAP was eluted with 10 mL of cold elution buffer (identical to binding buffer except 250 mM imidazole was added). All elution fractions were analyzed for the presence of protein using the Bradford dye reagent (Bio-Rad). All samples containing protein were combined and concentrated to ~8 mg/mL using the Centricon centrifugal concentration device, 10000 molecular weight cutoff (Millipore), and the expected molecular weight was confirmed by SDS−PAGE analysis.

T7 RNAP Transcription Runoff. All DNA used in the transcription process was purchased from Integrated DNA Technologies. The T7 template DNA oligo (5′-acg cac gct gta ata cga ctc act ata-3′) was annealed to either the RNA **I** (tetraloop) template (5′-mgmg cgc aca cgc gcc tat agt gag tcg tat tac agc gtg cgt-3′), RNA **II** (hexaloop) template (5′-mgmgc gct aca ctg cgc cta tag tga gtc gta tta cag cgt gcg t-3′), RNA **III** (heptaloop) template (5′-mgmgc gct act act gcg cct ata gtg agt cgt att aca gcg tgc gt-3′), or RNA **IV** (octaloop) template (5′-mgmgc gct act gac tgc gcc tat agt gag tcg tat tac agc gtg cgt-3′). All DNA templates used were purified by PAGE [20% acrylamide (29:1), 8 M urea gel] on a denaturing gel prior to use, and the molecular weights of the templates were validated by MALDI-MS.

All T7 transcription assays were performed on a 10 nmol scale. The T7 template and its corresponding RNA hairpin loop template were annealed by adding 10 nmol of each template to a 1.7 mL centrifuge tube containing 20 mM Tris, pH 8.0, 75 mM NaCl, and 0.5 mM EDTA, in a final volume of 1 mL. The 1.7 mL tube was incubated at 95 °C for 3 min followed by incubation on ice for 5 min. This 1.0 mL template mixture was added to a 40 mL centrifugation tube (Nalge Nunc: 3146−0050) containing a 9 mL solution of Tris, NTPs, etc., such that the final concentration in 10 mL is as follows: 40 mM Tris, pH 8.0, 10 mM $MgCl_2$, 10 mM DTT, 1 mM ATP, 1 mM GTP, 1 mM CTP, 1 mM UTP, 2 mM spermine, and 500 μL of T7 RNAP. The transcription reaction was then incubated at 37 °C for 6 h after which 100 μL of 500 mM EDTA, 3 mL of 4 M NaCl, and 30 mL of cold 100% EtOH were added to the transcription reaction. The contents were then incubated at −80 °C overnight. The following morning the tube was spun at 40000*g* for 30 min. The supernatant was discarded, and the pellet was washed with cold 70% ethanol. After a 1 h incubation at −80 °C, the crude product was centrifuged again at 40000*g* for 30 min. After decanting, the pellet was dried via lyophilization. After the pellet was dried completely, it was resuspended in a minimal volume (typically 300 μL) of 10 mM Tris and 0.5 mM EDTA, pH 7.5, and PAGE purified [20% acrylamide (29:1), 8 M urea gel, 2 mm thickness]. The molecular weights of all products were verified by MALDI-MS.

Isothermal Titration Calorimetry (ITC). ITC measurements were performed at 25 °C on a MicroCal VP-ITC (MicroCal, Inc., Northampton, MA). A standard experiment consisted of titrating 10 μL of a 500 μM ligand solution from a 250 μL syringe (rotating at 300 rpm) into the sample cell containing 1.42 mL of a 5 μM RNA solution. Each standard experiment was followed by a corresponding experiment where the ligand was titrated with buffer alone. The duration of injection was set to 20 s, and the delay between injections was 180 s. The initial delay prior to the first injection was 60 s. To derive the heat associated with each injection, the area under each heat burst curve (microcalories per second versus seconds) was determined by integration (using the Origin version 5.0 software; MicroCal, Inc., Northampton, MA). The heat associated with ligand solvation (ligand titrated with buffer) was subtracted from the corresponding heat associated with ligand−RNA injection to yield the heat due solely to ligand binding for each injection. The data fitting requirements were such that the thermodynamic parameters were derived from the curves that produced the lowest amount of deviation. In most cases fitting to a sequential site binding model of two or three binding sites gave the most accurate data. The additional sites are not detected in the Job plot analysis and likely represent low-affinity sites. Analogous low-affinity binding sites have previously been observed in the aminoglycoside−16S rRNA interaction (*43*). The buffer solution for the ITC experiments was 10 mM Tris (pH 7.5) and 0.1 mM EDTA. All RNAs utilized in ITC experiments were derived from T7 transcription runoff.

RESULTS

Size Specificity and Sequence Generality for the Binding of DOS Dimers to RNA. The determination of binding constants for small molecule−RNA interactions is a problem without a universal, generally applicable solution. A number of techniques have been developed for the determination of binding constants, such as displacement of a fluorescent ligand (*33*, *60*, *61*), gel shift (*62*), isothermal titration calorimetry (*63*, *64*), surface plasmon resonance (*65*, *66*), and electrospray ionization mass spectrometry (ESI-MS) (*67*). An alternative and convenient method is to use fluorescently labeled RNA, either with an unnatural base (*34*, *64*, *68*, *69*) or via end-label (*31*, *40*, *41*, *70*−*73*). When binding assays are performed with such fluorescently labeled RNAs, a dose-dependent, saturatable change in fluorescence is observed; such change in fluorescence is attributed to a conformational change in the RNA induced by the ligand upon complexation, which is often seen with small molecule−RNA interactions (*11*, *70*, *74*).

In our prior report, **B-12** demonstrated excellent affinity and selectivity for RNA octaloops as compared to all other secondary structures tested (*41*). In this current work **B-12** analogues were challenged in the same selectivity matrix; none of the **B-12** analogues display any selectivity for RNA hairpin loop size (see Figure 1B). The positional isomer **B-11** and pyridine containing **B-14** show little (2−3-fold) preference for hairpin size, and the mesitylene-based **B-13** exhibits no binding preference. It is interesting that a simple change in the projection of the DOS units off the aromatic ring leads to dramatic changes in specificity and affinity: **B-11** binds the octaloop sequences with >10-fold weaker affinity than **B-12**. The data suggest that not only are the hydrophobic/hydrophilic properties of **B-12** properly balanced for octaloop selectivity but also the geometric linkage of **B-12** is superior for targeting octaloops. As shown in Figure 1B these DOS dimers exhibit no sequence dependence for RNA hairpin loop binding, suggesting that these molecules are indeed general RNA hairpin loop binding compounds.

Determination of Specificity for Various RNA Secondary Structural Elements. Inside the cell, a RNA targeting small molecule will encounter a multitude of differing RNA

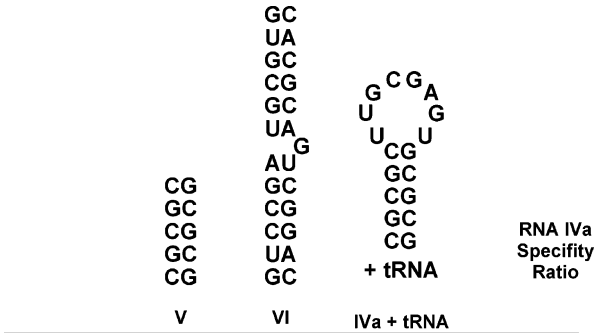

B-11	>30.0	4.85	1.82	0.90
B-12	>25.0*	>25.0*	0.17	1.13
B-13	6.07	14.95	10.08	21.0
B-14	14.17	6.70	2.26	1.01

FIGURE 2: Specificity of DOS dimers for different RNA secondary structures. All K_d values are listed in μM and were determined with the end-labeled method using the RNAs depicted with a fluorescein at their 3′ terminus. For RNAs **V** and **VI** (which are two strands that are annealed together) only one of the 3′ ends contains a fluorescein. The tRNA mixture is in 100-fold (base) excess to RNA **IVa**. The specificity ratio is defined as the (K_d in the presence of competitor tRNA)/(K_d in the absence of competitor tRNA) (*33*); thus the larger the specificity ratio above 1.0 the less specific a molecule is for the target RNA. The asterisk indicates that the data were previously reported (*41*).

structures. In order to assess the DOS dimers' structural specificity, a series of binding assays were performed against common RNA secondary structures and potential competitor RNAs (see Figure 2). In particular, the four DOS dimers had their binding to a fully base-paired stem (**V**) and a single base bulge (**VI**) assessed. In addition, their specificity for binding to octaloop **IVa** in the presence of a 100-fold excess of tRNA was evaluated. Compounds **B-11**, **B-12**, and **B-13** showed a 10-fold selectivity for the octaloop over the common GC stem (**V**). Both **B-12** and **B-13** are quite specific for octaloops over a single base RNA bulge (**VI**), whereas **B-11** is much less so (see Figures 1 and 2). Consistent with the results from Figure 1B, **B-14** was nonselective in its binding to all RNAs, yielding only a 2-fold selectivity for RNA **V** and no selectivity for RNA **VI**. These data suggest that, in the concentration range required for binding saturation, **B-11**, **B-12**, and **B-13** owe their observed affinity to hairpin loop binding rather than stem binding, while **B-14** may contact the stem region itself.

An excellent test of selectivity is to perform a binding assay in the presence of competitor tRNA (*33*), as tRNA may account for as much as 15% of the total concentration of cellular RNA (*13*). In this type of experiment, the target RNA is placed in the presence of a 100-fold base excess of *E. coli* tRNA, and the binding of the compound is examined. A specificity ratio [(K_d in the presence of competitor tRNA)/(K_d in the absence of competitor tRNA)] can then be calculated (*33*). The closer the specificity ratio is to 1, the more selective the binding is for the target RNA. The aminoglycosides have been shown to have specificity ratios ranging from 1.3 to 2.0 when assayed for binding to the Rev RNA (*33*). In this experiment, given the nonselective nature of **B-13**, it was not surprising to find a decrease in binding affinity for **B-13** with RNA **IVa**. In the presence of competitor tRNA the dissociation constant of **B-13** for

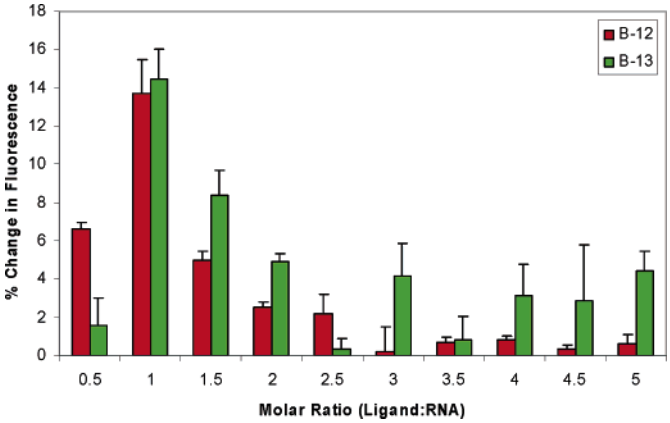

FIGURE 3: Determination of ligand binding stoichiometry as assessed by Job plots. During a Job plot assay the total molar concentration of ligand and RNA is kept constant, five times the K_d, while the ligand:RNA ratio is varied. The stoichiometry of binding is the molar ratio that shows the largest amount of binding. Job plots were constructed for **B-12** and **B-13** binding to RNA octaloop **IVa**. For both **B-12** and **B-13** a maximal change in fluorescence occurs at a molar ratio of 1:1; thus the stoichiometry of binding is taken to be 1:1. All error bars represent one standard deviation from the mean.

octaloop **IVa** was reduced by more than 20-fold. Quite surprisingly, **B-11** and **B-14**, which are equally nonselective, were able to bind to RNA **IVa** even in the presence of a 100-fold base excess of competitor tRNA, suggesting that tRNAs may not have appropriate binding sites for these DOS dimers. The binding of **B-12** to octaloop **IVa** was unaffected by the presence of competitor tRNA, consistent with previous results (*41*).

Determination of Binding Stoichiometry. The observed selectivity of **B-12** for RNA octaloops, in contrast to the more promiscuous **B-11**, **B-13**, and **B-14**, could arise from differences in binding stoichiometry. Two common methods to determine stoichiometry of binding are ESI-MS (*75*) and Job plots (*73*). Job plots present a convenient format if one has a highly robust binding assay (*76*), which the end-labeled method provides. In a Job plot the ligand:RNA molar ratio is varied while the total molar concentrations remain constant. The stoichiometry of binding is determined by the molar ratio where maximal binding is observed. Experiments to construct Job plots were carried out for compounds **B-12** and **B-13** binding to RNA **IVa**; **B-11** and **B-14** were omitted due to material constraints imposed by the Job plot that require that the total concentration of ligand and receptor be at least 5 times greater than the K_d (*76*). Through Job plot analysis it was determined that maximal binding response is found at a molar ratio of 1:1, which is indicative of a 1:1 binding stoichiometry (Figure 3). Thus it is reasonable to conclude that **B-12**'s RNA hairpin loop size selectivity is not the result of a unique stoichiometry of binding, as a nonselective analogue (**B-13**) exhibits the same binding stoichiometry.

Exploring the Role of Protonation-Coupled Binding. The electrostatic interactions between small molecules and RNA targets are an important criterion for binding and have been exploited as a means of enhancing affinity (*77*−*79*). Wang and Tor demonstrated that protonation states of individual amines are subtle contributors to the overall binding affinity of aminoglycoside−RNA interactions (*80*). Since then, Pilch and co-workers have extensively shown that the aminogly-

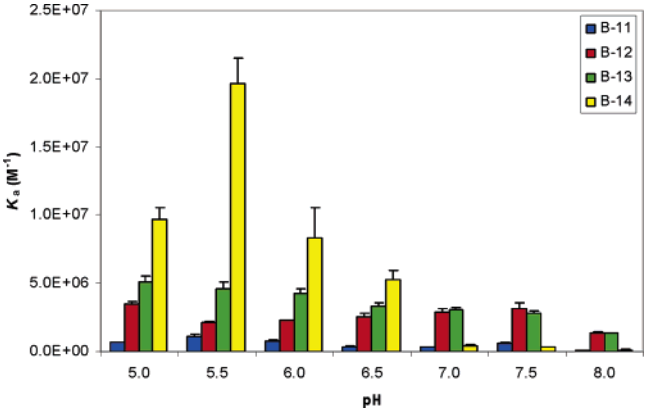

FIGURE 4: pH dependence studies to probe the contribution of protonation-induced binding. As electrostatics play a crucial role in RNA binding, the basicity of the amines can have a large impact on the binding affinity. The binding of the four DOS dimers to RNA octaloop **IVa** was assessed at a range of pH values. Compounds **B-11**, **B-12**, and **B-13** exhibit little or no dependence on pH in their binding to RNA **IVa**. The pH-dependent nature of **B-14** suggests that protonation of the pyridine nitrogen greatly enhances binding. Error bars reflect 95% confidence intervals.

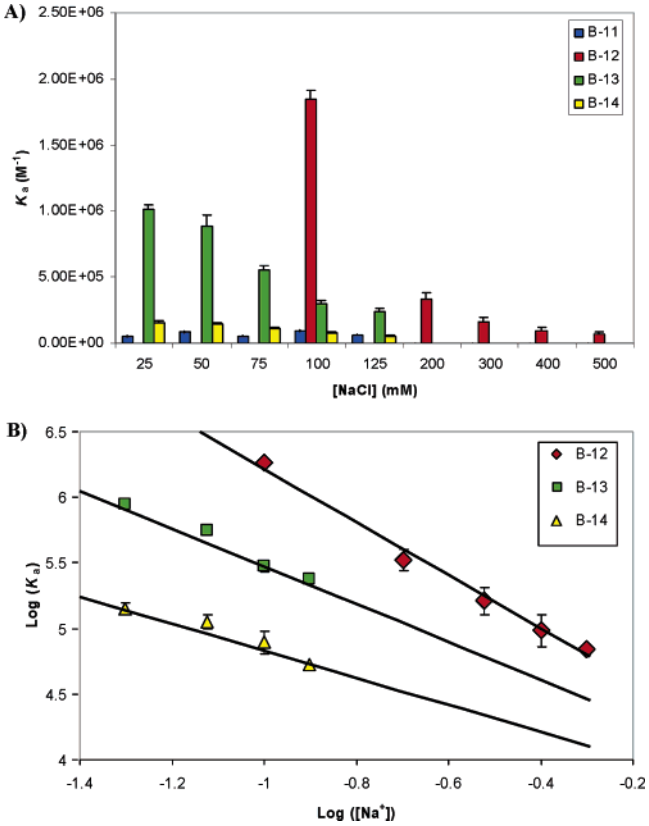

FIGURE 5: Dependence of DOS dimer−RNA binding affinity on ionic strength. (A) Graph depicting the ionic-dependent nature of **B-11**, **B-12**, **B-13**, and **B-14** binding RNA **IVa**. Error bars represent one standard deviation from the mean. (B) Graph depicting the linear relationship between the log(K_a) and log([Na^+]) in these same binding events. The slope of this line determines the $-Z\varphi$ and provides a lower limit estimate of the number of amine contacts with the RNA. All error bars represent 95% confidence intervals.

cosides exhibit a pH-dependent, or protonation-induced, binding to the A-site RNA (*42*−*44*, *64*, *81*, *82*). These studies have revealed pH-dependent binding to be a hallmark of aminoglycoside−RNA interactions (*44*).

We investigated whether the DOS dimers exhibit protonation-coupled binding and if such an event could be the reason for the observed selectivity of **B-12**. The dissociation constants, as assessed by the end-label binding assay at a range of pH values (5.0−8.0, at intervals of 0.5 pH unit), showed little to no change for **B-11**, **B-12**, and **B-13** with RNA **IVa** at the different pH values tested (Figure 4). This is perhaps not surprising as the amines on the 2-deoxystreptamine units should be fully protonated at all pH values from 5.0 to 8.0. As the protonation state of the 2-deoxystreptamines does not change in this pH range, no change in binding affinity would be expected. This is in contrast to the aminoglycosides, whose various amines have pK_a values that are quite different from one another and do exhibit pH-dependent RNA binding (*44*).

In contrast, **B-14** exhibited a steep pH-dependent binding, beginning at pH 6.5 and reaching maximal binding at pH 5.5; the affinity of **B-14** for octaloop **IVa** increased over 150-fold (K_d 7.99 μM at pH 8.0 to K_d 0.05 μM at pH 5.5) at lower pH values. The marked difference in binding affinity can likely be attributed to protonation of the pyridine nitrogen, whose pK_a in water is ~5.3. Compound **B-14** was then tested for pH-dependent, hairpin loop size selectivity by determining its dissociation constant with RNAs **I**, **II**, **III**, and **IV** at pH 5.5; however, even though strong binding affinity was retained (average $K_d = 0.23 \pm 0.07$ μM), no selectivity was observed (see Supporting Information).

Dependence of Binding on Ionic Strength. As described above, the observed selectivity of compound **B-12** for RNA octaloops does not appear to be the result of differing binding stoichiometries or a difference in protonation-coupled binding events. However, the selectivity could potentially be due to a difference in the number of electrostatic contacts made upon complexation. To provide insight into such molecular details, the end-label method was utilized in binding assays with varying concentrations of Na^+ in conjugation with van't Hoff analysis (Figure 5). The following relationship between dissociation constant and sodium concentration has previously been derived (*83*):

$$\frac{\partial \log(K_a)}{\partial \log([Na^+])} = -Z\varphi$$

where Z is the apparent change of the bound ligand and φ is the fraction of Na^+ bound per RNA phosphate group. The value for φ for the poly(rA)−poly(rU) duplex and single-stranded poly(rA) has been determined to be 0.89 and 0.78, respectively (*83*). As such, it has previously been assumed that an RNA containing single-stranded and duplex regions (such as an internal loops or hairpin loops) will likely have a intermediate value of φ (*44*).

Compounds **B-11**, **B-13**, and **B-14** were tested for their ability to bind RNA **IVa** in the presence of 25, 50, 75, 100, and 125 mM NaCl. Compound **B-12** was assayed for binding to RNA **IVa** in the presence of 100, 200, 300, 400, and 500 mM NaCl. **B-12** was tested at higher NaCl concentrations as **B-12**'s binding affinity did not change appreciably in the lower NaCl concentration range. The log of the K_a values derived from these experiments was then plotted against the log of the molar Na^+ concentration. The slope derived from the linear relationship between log(K_a) and log([Na^+]) provides a lower limit estimation of the number of amine contacts being made with the RNA. Compound **B-12** exhibits

Table 1: Calculated Free Energies of Binding in the Presence of 100 mM NaCl[a]

	ΔG_{total} (kcal/mol)	ΔG_{elec} (kcal/mol)
B-11	-6.7 ± 0.1	ND
B-12	-8.5 ± 0.1	-2.2 ± 0.1
B-13	-7.4 ± 0.1	-1.7 ± 0.1
B-14	-6.6 ± 0.1	-1.2 ± 0.1

[a] The total free energy of binding was determined by the relationship $\Delta G_{total} = -RT \ln(K_a)$. ΔG_{elec} was determined from analysis of the van't Hoff plots (see text).

a slope of -2.0 ± 0.1 in these experiments, which suggested that as few as two amines of this compound contact the RNA. Compounds **B-13** and **B-14** make at least one amine contact (slopes of -1.5 ± 0.1 and -1.1 ± 0.2, respectively). Binding of compound **B-11** showed a steep ionic dependence but failed to yield a linear dose-dependent relationship upon further increase of NaCl and could not be subjected to van't Hoff analysis. These studies provide our first insight into a possible reason for the observed selectivity of **B-12** for RNA octaloops: **B-12** exhibits the strongest electrostatic interactions with RNA **IVa**. The higher salt concentrations required to perform the van't Hoff analysis was an initial indication of the strength of the electrostatic interaction between **B-12** and RNA **IVa**. van't Hoff analysis confirmed that **B-12** likely makes more amine contacts with the RNA than either **B-13** or **B-14**.

The portion of the free energy associated with electrostatic interactions can be determined by the relationship:

$$\Delta G_{elec} = Z\varphi RT \ln([Na^+])$$

where $Z\varphi$ is the slope determined through linear regression analysis. The ΔG_{elec} for compounds **B-12**, **B-13**, and **B-14** were determined to be -2.2, -1.7, and -1.2 kcal/mol, respectively, when the Na^+ concentration is taken to 100 mM (see Table 1). The total free energy of binding can be derived from

$$\Delta G_{total} = -RT \ln(K_a)$$

where K_a is the association constant determined from the end-label method at 100 mM NaCl. Comparing the total free energy of binding with the electrostatic contribution, **B-12**, **B-13**, and **B-14** appear to only derive approximately one-quarter of their total free energy of binding from these electrostatic interactions in the presence of 100 mM Na^+ (Table 1). This low level of electrostatic contribution is in stark contrast to aminoglycoside−A-site interaction in which at least *half* of the total binding free energy comes from electrostatic contributions (*82*).

Thermodynamic Parameters As Assessed by Isothermal Titration Calorimetry. Isothermal titration calorimetry (ITC) has proven to be a valuable tool for understanding the thermodynamic parameters of ligand−macromolecule binding. Data such as K_a, ΔG, ΔH, ΔS, and ΔC_p can be determined from a series of ITC experiments. Because the biochemical experiments above were unable to provide a clear descriptor of selectivity, ITC was used in an effort to dissect the different thermodynamic parameters. The K_a values derived from ITC also offer an independent means to determine specificity of **B-12** for a given sized RNA hairpin loop.

Table 2: Thermodynamic Parameters As Determined by ITC[a]

	K_d (μM)	ΔG	ΔH	$T\Delta S$
		RNA **I**		
B-11	2.32 ± 0.1	-7.7 ± 0.1	-1.3 ± 0.2	6.4 ± 0.2
B-12	12.5 ± 0.6	-6.7 ± 0.1	-12.4 ± 0.2	-5.7 ± 0.1
B-13	0.18 ± 0.01	-9.1 ± 0.1	-1.8 ± 0.1	7.3 ± 0.1
B-14	3.99 ± 0.1	-7.3 ± 0.1	-1.1 ± 0.2	6.2 ± 0.1
		RNA **II**		
B-11	48.6 ± 8.0	-5.9 ± 0.1	-16.1 ± 0.7	-10.2 ± 0.6
B-12	33.2 ± 2.9	-6.1 ± 0.1	-19.6 ± 0.9	-13.5 ± 0.8
B-13	0.17 ± 0.01	-9.2 ± 0.1	-1.2 ± 0.2	8.0 ± 0.1
B-14	7.04 ± 2.6	-7.0 ± 0.2	-3.7 ± 0.6	3.3 ± 0.4
		RNA **III**		
B-11	6.4 ± 6.9	-7.1 ± 0.5	-11.6 ± 1.9	-4.5 ± 1.4
B-12	19.4 ± 0.1	-6.4 ± 0.1	-2.4 ± 0.6	4.0 ± 0.5
B-13	3.5 ± 0.6	-7.4 ± 0.1	-1.5 ± 0.2	5.9 ± 0.3
B-14	1.28 ± 0.1	-8.0 ± 0.1	-0.63 ± 0.4	7.4 ± 0.3
		RNA **IV**		
B-11	14.2 ± 1.1	-6.6 ± 0.1	-13.9 ± 0.2	-7.3 ± 0.2
B-12	0.8 ± 0.01	-8.3 ± 0.1	-1.4 ± 0.6	6.9 ± 0.5
B-13	0.5 ± 0.03	-8.5 ± 0.1	-1.1 ± 0.1	7.4 ± 0.1
B-14	5.6 ± 3.8	-7.1 ± 0.3	-2.4 ± 0.3	4.7 ± 0.1

[a] ΔG, ΔH, and $T\Delta S$ are listed in kcal/mol.

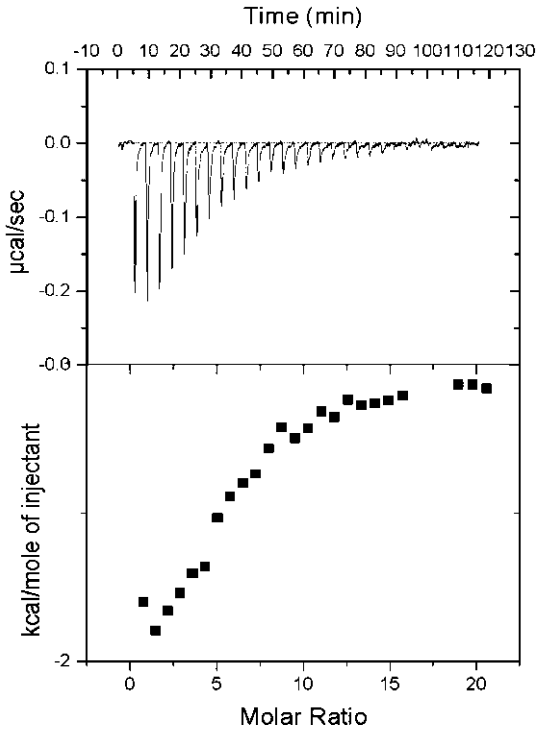

FIGURE 6: Determination of thermodynamic parameters by ITC. Shown is the titration of a solution of **B-12** into RNA **II** at pH 7.5.

ITC experiments were thus conducted with the four ligands and RNAs **I**, **II**, **III**, and **IV**. Recall that the end-labeled assay technique showed **B-12** to be a strong binder to RNA **IV** (octaloop; $K_d = 0.32$ μM) but to have considerably weaker binding affinity for RNA **I** (tetraloop), RNA **II** (hexaloop), and RNA **III** (heptaloop; $K_d = 9.9$ to >25 μM; see Figure 1B). The data from the ITC experiments are displayed in Table 2, and a representative ITC trace is shown in Figure 6. Importantly, the K_d values from ITC largely agree with those derived from the fluorescence binding assays and RNase footprinting (*41*). In all experimental methods, **B-12**

is selective for octaloop **IV** over all other loop sizes. From the ITC data, it would appear that $T\Delta S$ is an important contributor to **B-12**'s specificity as the entropic term is most favorable when binding to the octaloop (tightest binder) and most disfavored for binding the hexaloops (weakest binder). In fact, for all compounds tested the most favorable binding for a given compound against the series of RNAs is associated with the most favorable entropic contribution. This entropically driven binding event is unusual as the aminoglycosides binding to the 16S rRNA are driven by enthalpic association at physiological pH (*43*).

The lack of specificity of compound **B-13** can also be explained through the ITC data. When comparing the thermodynamic parameters of **B-12** and **B-13** for RNA **IV**, one finds that both compounds exhibit nearly identical enthalpic and entropic terms. However, **B-13** retains essentially constant enthalpic and entropic contributions when binding to the other hairpin loops. Conversely, the entropic contribution for **B-12** becomes a detriment when binding to smaller sized RNA hairpin loops. The nearly constant enthalpic and entropic contributions for the binding of **B-13** to all of the hairpin loops may explain the lack of selectivity of this compound. The thermodynamic profile of **B-11** and **B-14** for the series of hairpin loops reveals an inconsistent trend with respect to the entropic contribution, as **B-11** and **B-14** experience an enthalpic/entropic compensation when binding to the different hairpin loops while retaining a steady total free energy of binding.

DISCUSSION

There is an escalating interest in small molecule−RNA binding, both for fundamental biochemical studies and for medicinal applications. Beyond the ribosome, several RNAs have been suggested as targets for therapeutic intervention. The general development of small molecules that target 5′-UTRs has gained momentum (*84*, *85*) and has met with various degrees success in vivo (*30*, *31*). Disruptors of RNA−protein interactions have been sought for combating HIV (*86*, *87*), while interfering with RNA−RNA interactions has led to the development of a novel antibacterial strategy (*31*, *73*). Additionally, the discovery of catalytic RNA has enabled the use of small molecules to target these unique active sites (*88*−*93*).

A standing challenge is to fully derive rules governing small molecule−RNA binding, such that structural- and sequence-specific ligands can be designed from first principles. However, targeting RNA with any degree of specificity has proven to be a demanding task. In an effort to develop the requisite specificity suitable for targeting RNAs in vivo, we envision a series of small molecule "modules" that are specific for the various types of RNA secondary structures. We thus seek to develop small molecules specific for RNA hairpin loops, others that selectively bind internal loops, and still others that recognize bulged regions. As (for moderately sized RNAs) RNA secondary structure can reliably be determined from its primary sequence (*94*), such a modular approach could allow any RNA to be targeted through linkage of appropriate modules.

In a first step we previously disclosed a class of small molecules, dimers of 2-deoxystreptamine (DOS dimers), which are able to bind to RNA hairpin loops (*40*). In a subsequent effort DOS dimers that displayed specificity for hairpin loop size were discovered (*41*). As this level of specificity for a RNA hairpin loop of a given size was unprecedented, we sought to understand the origins of this specificity by performing a series of biochemical and biophysical assays with **B-12** (a compound highly specific for RNA octaloops) and structurally related derivatives.

Initially, a matrix of binding assays was designed to test the degree of size specificity, as well as to assess sequence preference. The RNAs utilized in the matrix include four RNA hairpin loops that are similar in sequence but vary in size, as well as a collection of tetra-, hepta-, and octaloops to assess sequence generality. The results from individual binding assays for each ligand against each RNA demonstrated that indeed **B-12** is the lone compound that binds to RNA hairpin loops with any size specificity. Additional assays conducted revealed that neither differences in binding stoichiometry nor influence of ligand protonation could account for the observed specificity; all compounds tested yielded a 1:1 stoichiometry of binding, and their binding to RNA was either pH-independent (**B-11**, **B-12**, and **B-13**) or the pH dependence did not confer selectivity (**B-14**). Though these assays were unable to provide an explanation of the observed hairpin loop size selectivity, it was confirmed that the DOS dimers tested exhibit little to no primary sequence dependence in their RNA binding and can thus be considered general RNA hairpin loop binding modules.

Binding assays with varying concentrations of Na^+ followed by van't Hoff analysis allowed for a calculation of a lower limit estimate of the number of amines making contact with the RNA upon complexation. Interestingly, **B-12** makes the greatest number of amine contacts, suggesting a greater electrostatic contribution for **B-12** in its binding to RNA. By varying the ionic strength, the electronegative RNA is masked by the abundance of Na^+; hence a compound whose binding is dependent on electrostatic interactions will have a decreased affinity as the ionic strength increases. Of the compounds tested, higher concentrations of Na^+ were required to significantly affect the binding of **B-12** to RNA **IVa**. Thus, these ionic-dependence studies revealed that **B-12** likely makes the greatest number of electrostatic contacts and these electrostatic interactions contributed only ∼25% of its total binding energy.

Further insights into the DOS dimer−RNA interactions were gained through ITC experiments; ITC has proven to be a valuable tool in dissecting aminoglycoside−RNA interactions (*42*−*44*, *64*, *81*, *82*). The ITC experiments confirm the binding specificity and binding affinities for the DOS dimers that were initially determined from the end-label method. Interestingly, the general trend emerged that favorable binding was associated with high entropic contributions. **B-12** was the only compound tested whose entropic contribution to the total free energy of binding changed significantly depending on the size of the RNA hairpin loop. This is likely a factor in the observed selectivity of **B-12** for RNA hairpin octaloops: **B-12** makes the greatest number of electrostatic contacts, which may result in a favorable entropy due to cation release. Cation release is a common event in small molecule−nucleic acid interactions (*95*, *96*).

The results uncovered during the course of this investigation reveal a binding profile for the DOS dimers that is quite unlike that of the aminoglycosides. pH-dependent binding

is a signature of aminoglycoside−RNA interactions (*44*); however, the majority of the compounds tested in this study do not show such a pH dependence. The electrostatic contribution to binding was severely reduced for the DOS dimers as compared to their aminoglycoside counterparts (*59*, *82*). Thermodynamic analysis suggests that in order for the DOS dimers to bind favorably there tends to be an associated high entropic contribution. This entropic factor is not observed for the aminoglycoside−RNA binding; rather, enthalpic factors make up the majority of the binding energy in these cases (*82*). It is not clear at this time if the low enthalpic contribution is an intrinsic feature of the DOS dimer−RNA binding or a general necessity for small molecules that bind RNA hairpin loops; future experiments are being designed to address this issue.

The structure−activity relationship (SAR) between the various DOS dimers tested in this study reveals an unforgiving profile with regard to RNA octaloop selectivity. All structural deviations from **B-12** resulted in the loss of RNA octaloop selectivity, and in the majority of cases these deviations also resulted in a loss of affinity for RNA octaloops. Numerous factors appear to be important for strong binding of DOS dimers to RNA hairpin loops. Hydrophobic interactions appear to enhance affinity, as **B-13** retained binding affinities in the mid-nanomolar range for all hairpin loops tested. Also, protonation-coupled binding can enhance affinity markedly, as in the case of **B-14**, but this was neither a general phenomenon (as the other linkers lacked ionizable functional groups) nor did such coupling lead to selectivity. **B-12** appears to be the only compound in which the entropic contribution to the binding affinity varies with hairpin loop size: for octaloops, the entropic parameter is strongly positive and hence provides a considerable driving force for binding, whereas for the smaller RNA hairpin loops, the entropic parameter becomes negative and is a detriment to strong RNA binding. It is not immediately apparent from the SAR how the structure of **B-12** leads to these entropic differences. Ultimately, structural studies, in conjugation with molecular modeling, will be necessary for a comprehensive view of these interactions.

This study confirms that compound **B-12** binds to RNA octaloops with high affinity and specificity. It also suggests that favorable entropy of binding can partially explain this binding preference, a somewhat surprising notion based on the known enthalpic contributions in the binding of aminoglycosides to RNA. It may thus be possible to design next generation compounds that are predisposed for binding to a RNA hairpin loop of a given size, and this may lead to a family of compounds, each of which is specific for a RNA hairpin loop of a certain size. Although less common than smaller loop sizes, RNA octaloops do exist in nature, as exemplified by the hepatitis C IRES (loop **VIa** in Figure 1B). The relative paucity of octaloops suggests that they could be targeted in a specific manner by small molecules. Only after a comprehensive set of rules for small molecule−RNA binding is fully elucidated can one begin to systematically target any RNA in the cell with small molecules.

SUPPORTING INFORMATION AVAILABLE

Full binding curves and all ITC data. This material is available free of charge via the Internet at http://pubs.acs.org.

REFERENCES

1. Hajduk, P. J., Huth, J. R., and Tse, C. (2005) Predicting protein druggability, *Drug Discov. Today 10*, 1675−1682.
2. Hopkins, A. L., and Groom, C. R. (2002) The druggable genome, *Nat. Rev. Drug Discov. 1*, 727−730.
3. Russ, A. P., and Lampel, S. (2005) The druggable genome: an update, *Drug Discov. Today 10*, 1607−1610.
4. Dervan, P. B., Doss, R. M., and Marques, M. A. (2005) Programmable DNA binding oligomers for control of transcription, *Curr. Med. Chem. Anticancer Agents 5*, 373−387.
5. Dervan, P. B., and Edelson, B. S. (2003) Recognition of the DNA minor groove by pyrrole-imidazole polyamides, *Curr. Opin. Struct. Biol. 13*, 284−299.
6. Dervan, P. B., and Burli, R. W. (1999) Sequence-specific DNA recognition by polyamides, *Curr. Opin. Chem. Biol. 3*, 688−693.
7. Wemmer, D. E., and Dervan, P. B. (1997) Targeting the minor groove of DNA, *Curr. Opin. Struct. Biol. 7*, 355−361.
8. Best, T. P., Edelson, B. S., Nickols, N. G., and Dervan, P. B. (2003) Nuclear localization of pyrrole-imidazole polyamide-fluorescein conjugates in cell culture, *Proc. Natl. Acad. Sci. U.S.A. 100*, 12063−12068.
9. Belitsky, J. M., Leslie, S. J., Arora, P. S., Beerman, T. A., and Dervan, P. B. (2002) Cellular uptake of N-methylpyrrole/N-methylimidazole polyamide-dye conjugates, *Bioorg. Med. Chem. 10*, 3313−3318.
10. Cheng, A. C., Calabro, V., and Frankel, A. D. (2001) Design of RNA-binding proteins and ligands, *Curr. Opin. Struct. Biol. 11*, 478−484.
11. Hermann, T. (2002) Rational ligand design for RNA: the role of static structure and conformational flexibility in target recognition, *Biochimie 84*, 869−875.
12. Sucheck, S. J., and Wong, C. H. (2000) RNA as a target for small molecules, *Curr. Opin. Chem. Biol. 4*, 678−686.
13. Tor, Y. (2003) Targeting RNA with small molecules, *ChemBioChem 4*, 998−1007.
14. Vicens, Q., and Westhof, E. (2003) RNA as a drug target: the case of aminoglycosides, *ChemBioChem 4*, 1018−1023.
15. Chow, C. S., and Bogdan, F. M. (1997) A structural basis for RNA−ligand interactions, *Chem. Rev. 97*, 1489−1514.
16. Tucker, B. J., and Breaker, R. R. (2005) Riboswitches as versatile gene control elements, *Curr. Opin. Struct. Biol. 15*, 342−348.
17. Winkler, W. C., and Breaker, R. R. (2005) Regulation of bacterial gene expression by riboswitches, *Annu. Rev. Microbiol. 59*, 487−517.
18. Epshtein, V., Mironov, A. S., and Nudler, E. (2003) The riboswitch-mediated control of sulfur metabolism in bacteria, *Proc. Natl. Acad. Sci. U.S.A. 100*, 5052−5056.
19. Grundy, F. J., Lehman, S. C., and Henkin, T. M. (2003) The L box regulon: lysine sensing by leader RNAs of bacterial lysine biosynthesis genes, *Proc. Natl. Acad. Sci. U.S.A. 100*, 12057−12062.
20. Mandal, M., Boese, B., Barrick, J. E., Winkler, W. C., and Breaker, R. R. (2003) Riboswitches control fundamental biochemical pathways in Bacillus subtilis and other bacteria, *Cell 113*, 577−586.
21. Mandal, M., and Breaker, R. R. (2004) Adenine riboswitches and gene activation by disruption of a transcription terminator, *Nat. Struct. Mol. Biol. 11*, 29−35.
22. Mandal, M., Lee, M., Barrick, J. E., Weinberg, Z., Emilsson, G. M., Ruzzo, W. L., and Breaker, R. R. (2004) A glycine-dependent riboswitch that uses cooperative binding to control gene expression, *Science 306*, 275−279.
23. McDaniel, B. A., Grundy, F. J., Artsimovitch, I., and Henkin, T. M. (2003) Transcription termination control of the S box system: direct measurement of S-adenosylmethionine by the leader RNA, *Proc. Natl. Acad. Sci. U.S.A. 100*, 3083−3088.
24. Nahvi, A., Barrick, J. E., and Breaker, R. R. (2004) Coenzyme B12 riboswitches are widespread genetic control elements in prokaryotes, *Nucleic Acids Res. 32*, 143−150.
25. Nahvi, A., Sudarsan, N., Ebert, M. S., Zou, X., Brown, K. L., and Breaker, R. R. (2002) Genetic control by a metabolite binding mRNA, *Chem. Biol. 9*, 1043.
26. Winkler, W. C., Cohen-Chalamish, S., and Breaker, R. R. (2002) An mRNA structure that controls gene expression by binding FMN, *Proc. Natl. Acad. Sci. U.S.A. 99*, 15908−15913.
27. Winkler, W. C., Nahvi, A., Roth, A., Collins, J. A., and Breaker, R. R. (2004) Control of gene expression by a natural metabolite-responsive ribozyme, *Nature 428*, 281−286.

28. Winkler, W. C., Nahvi, A., Sudarsan, N., Barrick, J. E., and Breaker, R. R. (2003) An mRNA structure that controls gene expression by binding S-adenosylmethionine, *Nat. Struct. Biol. 10*, 701−707.
29. Begg, E. J., and Barclay, M. L. (1995) Aminoglycosides−50 years on, *Br. J. Clin. Pharmacol. 39*, 597−603.
30. Werstuck, G., and Green, M. R. (1998) Controlling gene expression in living cells through small molecule-RNA interactions, *Science 282*, 296−298.
31. DeNap, J. C. B., Thomas, J. R., Musk, D. J., and Hergenrother, P. J. (2004) Combating drug-resistant bacteria: Small molecule mimics of plasmid incompatibility as antiplasmid compounds, *J. Am. Chem. Soc. 126*, 15402−15404.
32. Alper, P. B., Hendrix, M., Sears, P., and Wong, C. H. (1998) Probing the specificity of aminoglycoside-ribosomal RNA interactions with designed synthetic analogs, *J. Am. Chem. Soc. 120*, 1965−1978.
33. Luedtke, N. W., Liu, Q., and Tor, Y. (2003) RNA-ligand interactions: affinity and specificity of aminoglycoside dimers and acridine conjugates to the HIV-1 Rev response element, *Biochemistry 42*, 11391−11403.
34. Blount, K. F., and Tor, Y. (2003) Using pyrene-labeled HIV-1 TAR to measure RNA-small molecule binding, *Nucleic Acids Res. 31*, 5490−5500.
35. Tok, J. B., Cho, J., and Rando, R. R. (1999) Aminoglycoside antibiotics are able to specifically bind the 5′-untranslated region of thymidylate synthase messenger RNA, *Biochemistry 38*, 199−206.
36. Hermann, T. (2003) Chemical and functional diversity of small molecule ligands for RNA, *Biopolymers 70*, 4−18.
37. Verhelst, S. H. L., Michiels, P. J. A., van der Marel, G. A., van Boeckel, C. A. A., and van Boom, J. H. (2004) Surface plasmon resonance evaluation of various aminoglycoside-RNA hairpin interactions reveals low degree of selectivity, *ChemBioChem. 5*, 937−942.
38. Mei, H. Y., Cui, M., Heldsinger, A., Lemrow, S. M., Loo, J. A., Sannes-Lowery, K. A., Sharmeen, L., and Czarnik, A. W. (1998) Inhibitors of protein-RNA complexation that target the RNA: specific recognition of human immunodeficiency virus type 1 TAR RNA by small organic molecules, *Biochemistry 37*, 14204−14212.
39. Yan, Z., and Baranger, A. M. (2004) Binding of an aminoacridine derivative to a GAAA RNA tetraloop, *Bioorg. Med. Chem. Lett. 14*, 5889−5893.
40. Liu, X., Thomas, J. R., and Hergenrother, P. J. (2004) Deoxystreptamine dimers bind to RNA hairpin loops, *J. Am. Chem. Soc. 126*, 9196−9197.
41. Thomas, J. R., Liu, X., and Hergenrother, P. J. (2005) Size-specific ligands for RNA hairpin loops, *J. Am. Chem. Soc. 127*, 12434−12435.
42. Kaul, M., Barbieri, C. M., Kerrigan, J. E., and Pilch, D. S. (2003) Coupling of drug protonation to the specific binding of aminoglycosides to the A site of 16 S rRNA: elucidation of the number of drug amino groups involved and their identities, *J. Mol. Biol. 326*, 1373−1387.
43. Kaul, M., and Pilch, D. S. (2002) Thermodynamics of aminoglycoside-rRNA recognition: the binding of neomycin-class aminoglycosides to the A site of 16S rRNA, *Biochemistry 41*, 7695−7706.
44. Pilch, D. S., Kaul, M., Barbieri, C. M., and Kerrigan, J. E. (2003) Thermodynamics of aminoglycoside-rRNA recognition, *Biopolymers 70*, 58−79.
45. Fourmy, D., Recht, M. I., Blanchard, S. C., and Puglisi, J. D. (1996) Structure of the A site of Escherichia coli 16S ribosomal RNA complexed with an aminoglycoside antibiotic, *Science 274*, 1367−1371.
46. Brodersen, D. E., Clemons, W. M., Jr., Carter, A. P., Morgan-Warren, R. J., Wimberly, B. T., and Ramakrishnan, V. (2000) The structural basis for the action of the antibiotics tetracycline, pactamycin, and hygromycin B on the 30S ribosomal subunit, *Cell 103*, 1143−1154.
47. Carter, A. P., Clemons, W. M., Brodersen, D. E., Morgan-Warren, R. J., Wimberly, B. T., and Ramakrishnan, V. (2000) Functional insights from the structure of the 30S ribosomal subunit and its interactions with antibiotics, *Nature 407*, 340−348.
48. Vicens, Q., and Westhof, E. (2001) Crystal structure of paromomycin docked into the eubacterial ribosomal decoding A site, *Structure 9*, 647−658.
49. Vicens, Q., and Westhof, E. (2002) Crystal structure of a complex between the aminoglycoside tobramycin and an oligonucleotide containing the ribosomal decoding a site, *Chem. Biol. 9*, 747−755.
50. Vicens, Q., and Westhof, E. (2003) Crystal structure of geneticin bound to a bacterial 16S ribosomal RNA A site oligonucleotide, *J. Mol. Biol. 326*, 1175−1188.
51. Varani, G. (1995) Exceptionally stable nucleic acid hairpins, *Annu. Rev. Biophys. Biomol. Struct. 24*, 379−404.
52. Hall, K. B., and Williams, D. J. (2004) Dynamics of the IRE RNA hairpin loop probed by 2-aminopurine fluorescence and stochastic dynamics simulations, *RNA 10*, 34−47.
53. Hall, K. B. (1994) Interaction of RNA hairpins with the human U1A N-terminal RNA binding domain, *Biochemistry 33*, 10076−10088.
54. Gregorian, R. S., Jr., and Crothers, D. M. (1995) Determinants of RNA hairpin loop-loop complex stability, *J. Mol. Biol. 248*, 968−984.
55. Haasnoot, C. A., Hilbers, C. W., van der Marel, G. A., van Boom, J. H., Singh, U. C., Pattabiraman, N., and Kollman, P. A. (1986) On loop folding in nucleic acid hairpin-type structures, *J. Biomol. Struct. Dyn. 3*, 843−857.
56. Varani, G., Cheong, C., and Tinoco, I., Jr. (1991) Structure of an unusually stable RNA hairpin, *Biochemistry 30*, 3280−3289.
57. Abramovitz, D. L., and Pyle, A. M. (1997) Remarkable morphological variability of a common RNA folding motif: the GNRA tetraloop-receptor interaction, *J. Mol. Biol. 266*, 493−506.
58. Proctor, D. J., Schaak, J. E., Bevilacqua, J. M., Falzone, C. J., and Bevilacqua, P. C. (2002) Isolation and characterization of a family of stable RNA tetraloops with the motif YNMG that participate in tertiary interactions, *Biochemistry 41*, 12062−12075.
59. Jin, E., Katritch, V., Olson, W. K., Kharatisvili, M., Abagyan, R., and Pilch, D. S. (2000) Aminoglycoside binding in the major groove of duplex RNA: the thermodynamic and electrostatic forces that govern recognition, *J. Mol. Biol. 298*, 95−110.
60. Ryu, D. H., and Rando, R. R. (2001) Aminoglycoside binding to human and bacterial A-site rRNA decoding region constructs, *Bioorg. Med. Chem. 9*, 2601−2608.
61. Ryu, D. H., Litovchick, A., and Rando, R. R. (2002) Stereospecificity of aminoglycoside-ribosomal interactions, *Biochemistry 41*, 10499−10509.
62. Xiao, G., Kumar, A., Li, K., Rigl, C. T., Bajic, M., Davis, T. M., Boykin, D. W., and Wilson, W. D. (2001) Inhibition of the HIV-1 rev-RRE complex formation by unfused aromatic cations, *Bioorg. Med. Chem. 9*, 1097−1113.
63. Arya, D. P., Coffee, R. L., Jr., and Xue, L. (2004) From triplex to B-form duplex stabilization: reversal of target selectivity by aminoglycoside dimers, *Bioorg. Med. Chem. Lett. 14*, 4643−4646.
64. Kaul, M., Barbieri, C. M., and Pilch, D. S. (2004) Fluorescence-based approach for detecting and characterizing antibiotic-induced conformational changes in ribosomal RNA: comparing aminoglycoside binding to prokaryotic and eukaryotic ribosomal RNA sequences, *J. Am. Chem. Soc. 126*, 3447−3453.
65. Verhelst, S. H., Michiels, P. J., van der Marel, G. A., van Boeckel, C. A., and van Boom, J. H. (2004) Surface plasmon resonance evaluation of various aminoglycoside-RNA hairpin interactions reveals low degree of selectivity, *ChemBioChem. 5*, 937−942.
66. Agnelli, F., Sucheck, S. J., Marby, K. A., Rabuka, D., Yao, S. L., Sears, P. S., Liang, F. S., and Wong, C. H. (2004) Dimeric aminoglycosides as antibiotics, *Angew. Chem., Int. Ed. Engl. 43*, 1562−1566.
67. Swayze, E. E., Jefferson, E. A., Sannes-Lowery, K. A., Blyn, L. B., Risen, L. M., Arakawa, S., Osgood, S. A., Hofstadler, S. A., and Griffey, R. H. (2002) SAR by MS: a ligand based technique for drug lead discovery against structured RNA targets, *J. Med. Chem. 45*, 3816−3819.
68. Bradrick, T. D., and Marino, J. P. (2004) Ligand-induced changes in 2-aminopurine fluorescence as a probe for small molecule binding to HIV-1 TAR RNA, *RNA 10*, 1459−1468.
69. Wickiser, J. K., Cheah, M. T., Breaker, R. R., and Crothers, D. M. (2005) The kinetics of ligand binding by an adenine-sensing riboswitch, *Biochemistry 44*, 13404−13414.
70. Llano-Sotelo, B., and Chow, C. S. (1999) RNA-aminoglycoside antibiotic interactions: fluorescence detection of binding and conformational change, *Bioorg. Med. Chem. Lett. 9*, 213−216.
71. Haddad, J., Kotra, L. P., Llano-Sotelo, B., Kim, C., Azucena, E. F., Jr., Liu, M., Vakulenko, S. B., Chow, C. S., and Mobashery, S. (2002) Design of novel antibiotics that bind to the ribosomal acyltransfer site, *J. Am. Chem. Soc. 124*, 3229−3237.

72. Tok, J. B., Bi, L., and Saenz, M. (2005) Specific recognition of napthyridine-based ligands toward guanine-containing bulges in RNA duplexes and RNA-DNA heteroduplexes, *Bioorg. Med. Chem. Lett. 15*, 827−831.
73. Thomas, J. R., DeNap, J. B. C., Wong, M. L., and Hergenrother, P. J. (2005) The relationship between aminoglycosides' RNA binding proclivity and their antiplasmid effect on an IncB plasmid, *Biochemistry 44*, 6800−6808.
74. Leulliot, N., and Varani, G. (2001) Current topics in RNA-protein recognition: control of specificity and biological function through induced fit and conformational capture, *Biochemistry 40*, 7947−7956.
75. Sannes-Lowery, K. A., Griffey, R. H., and Hofstadler, S. A. (2000) Measuring dissociation constants of RNA and aminoglycoside antibiotics by electrospray ionization mass spectrometry, *Anal. Biochem. 280*, 264−271.
76. Huang, C. Y. (1982) Determination of binding stoichiometry by the continuous variation method: the Job plot, *Methods Enzymol. 87*, 509−525.
77. Baker, T. J., Luedtke, N. W., Tor, Y., and Goodman, M. (2000) Synthesis and anti-HIV activity of guanidinoglycosides, *J. Org. Chem. 65*, 9054−9058.
78. Boer, J., Blount, K. F., Luedtke, N. W., Elson-Schwab, L., and Tor, Y. (2005) RNA-selective modification by a platinum(II) complex conjugated to amino- and guanidinoglycosides, *Angew. Chem., Int. Ed. Engl. 44*, 927−932.
79. Luedtke, N. W., Carmichael, P., and Tor, Y. (2003) Cellular uptake of aminoglycosides, guanidinoglycosides, and poly-arginine, *J. Am. Chem. Soc. 125*, 12374−12375.
80. Wang, H., and Tor, Y. (1997) Electrostatic interactions in RNA aminoglycosides binding, *J. Am. Chem. Soc. 119*, 8734−8735.
81. Kaul, M., Barbieri, C. M., and Pilch, D. S. (2006) Aminoglycoside-induced reduction in nucleotide mobility at the ribosomal RNA A-site as a potentially key determinant of antibacterial activity, *J. Am. Chem. Soc. 128*, 1261−1271.
82. Kaul, M., Barbieri, C. M., and Pilch, D. S. (2005) Defining the basis for the specificity of aminoglycoside-rRNA recognition: a comparative study of drug binding to the A sites of Escherichia coli and human rRNA, *J. Mol. Biol. 346*, 119−134.
83. Record, M. T., Jr., Anderson, C. F., and Lohman, T. M. (1978) Thermodynamic analysis of ion effects on the binding and conformational equilibria of proteins and nucleic acids: the roles of ion association or release, screening, and ion effects on water activity, *Q. Rev. Biophys. 11*, 103−178.
84. Seth, P. P., Miyaji, A., Jefferson, E. A., Sannes-Lowery, K. A., Osgood, S. A., Propp, S. S., Ranken, R., Massire, C., Sampath, R., Ecker, D. J., Swayze, E. E., and Griffey, R. H. (2005) SAR by MS: discovery of a new class of RNA-binding small molecules for the hepatitis C virus: internal ribosome entry site IIA subdomain, *J. Med. Chem. 48*, 7099−7102.
85. Tibodeau, J. D., Fox, P. M., Ropp, P. A., Theil, E. C., and Thorp, H. H. (2006) The up-regulation of ferritin expression using a small-molecule ligand to the native mRNA, *Proc. Natl. Acad. Sci. U.S.A. 103*, 253−257.
86. Cho, J., and Rando, R. R. (1999) Specificity in the binding of aminoglycosides to HIV-RRE RNA, *Biochemistry 38*, 8548−8554.
87. Wang, S., Huber, P. W., Cui, M., Czarnik, A. W., and Mei, H. Y. (1998) Binding of neomycin to the TAR element of HIV-1 RNA induces dissociation of Tat protein by an allosteric mechanism, *Biochemistry 37*, 5549−5557.
88. von Ahsen, U., Davies, J., and Schroeder, R. (1991) Antibiotic inhibition of group I ribozyme function, *Nature 353*, 368−370.
89. Stage, T. K., Hertel, K. J., and Uhlenbeck, O. C. (1995) Inhibition of the hammerhead ribozyme by neomycin, *RNA 1*, 95−101.
90. Rogers, J., Chang, A. H., von Ahsen, U., Schroeder, R., and Davies, J. (1996) Inhibition of the self-cleavage reaction of the human hepatitis delta virus ribozyme by antibiotics, *J. Mol. Biol. 259*, 916−925.
91. Earnshaw, D. J., and Gait, M. J. (1998) Hairpin ribozyme cleavage catalyzed by aminoglycoside antibiotics and the polyamine spermine in the absence of metal ions, *Nucleic Acids Res. 26*, 5551−5561.
92. Zapp, M. L., Stern, S., and Green, M. R. (1993) Small molecules that selectively block RNA binding of HIV-1 Rev protein inhibit Rev function and viral production, *Cell 74*, 969−978.
93. Mikkelsen, N. E., Brannvall, M., Virtanen, A., and Kirsebom, L. A. (1999) Inhibition of RNase P RNA cleavage by aminoglycosides, *Proc. Natl. Acad. Sci. U.S.A. 96*, 6155−6160.
94. Mathews, D. H., Disney, M. D., Childs, J. L., Schroeder, S. J., Zuker, M., and Turner, D. H. (2004) Incorporating chemical modification constraints into a dynamic programming algorithm for prediction of RNA secondary structure, *Proc. Natl. Acad. Sci. U.S.A. 101*, 7287−7292.
95. Chaires, J. B. (1996) Dissecting the free energy of drug binding to DNA, *Anticancer Drug Des. 11*, 569−580.
96. Chaires, J. B. (1998) Drug−DNA interactions, *Curr. Opin. Struct. Biol. 8*, 314−320.

BI0607296